Published in final edited form as:
Stroke. 2012 April ; 43(4): 1115–1122. doi:10.1161/STROKEAHA.111.643080.

Myelin loss associated with neuroinflammation in hypertensive rats

Fakhreya Yousuf Jalal, PhD[1], **Yi Yang, PhD MD**[1], **Jeffrey Thompson, BS**[1], **Anita Claudine Lopez, MS**[1], and **Gary A. Rosenberg, MD**[1,2,3]

[1]Department of Neurology, University of New Mexico Health Sciences Center, Albuquerque, NM, 87131 USA

[2]Department of Neuroscience, University of New Mexico Health Sciences Center, Albuquerque, NM, 87131 USA

[3]Department of Cell Biology and Physiology, University of New Mexico Health Sciences Center, Albuquerque, NM, 87131 USA

Abstract

Background and purpose—Small vessel disease is the major cause of white matter injury in patients with vascular cognitive impairment. Matrix metalloproteinase (MMP)-mediated inflammation may be involved in the white matter damage with oligodendrocyte (Ol) death. Therefore, we used spontaneously hypertensive stroke-prone rats (SHR-SP) to study the role of neuroinflammation in white matter damage.

Methods—Permanent unilateral carotid artery occlusion (UCAO) was performed at 12-weeks of age in SHR-SP. Following surgery, rats were placed on a Japanese permissive diet (JPD) and received 1 % NaCl in drinking water. MRI, histology, biochemistry, and ELISA characterized white matter lesions and cognitive impairment was tested by Morris water maze (MWM).

Results—white matter damage was observed 4-5 weeks following UCAO/JPD. Immunoblotting showed marked reduction in myelin basic protein (MBP) and up regulation of immature Ols. Mature Ols underwent caspase-3-mediated apoptosis. MWM showed cognitive impairment. Abnormally appearing vessels were observed and surrounded by inflammatory-like cells. IgG extravasation and hemorrhage, indicating blood-brain barrier (BBB) disruption, was closely associated with MMP-9 expression. Lesions in white matter showed reactive astrocytosis and activated microglia that expressed tumor necrosis factor-α (TNF-α). MMP-3 and MMP-9 were significantly increased and MMP-2 reduced in astrocytes and Ol.

Conclusion—We found apoptosis of mature Ols with an increase in immature Ols. Increased MMP-3, MMP-9 and TNF-α were associated with myelin breakdown and BBB disruption. Neuroinflammation is an important factor in white matter damage and Ol death, and studies using this new model can be done to assess agents to block inflammation.

Address Correspondence to: Gary A. Rosenberg, M.D., Department of Neurology, MSC10 5620, 1 University of New Mexico, Albuquerque, NM 87131-0001, Tel: +1-505-272-3315, FAX: +1-505-272-6692, grosenberg@salud.unm.edu.

Disclosures: None.

Keywords

White matter; vascular cognitive impairment; Matrix metalloproteinases

Introduction

Vascular cognitive impairment is a heterogeneous disease due to large and small vessel disease. [1] White matter injury is commonly seen in small vessel disease with arteriolosclerosis secondary to hypertension and diabetes. [2] As the population increases in age, the incidence of vascular causes of dementia is projected to rise, creating a need for animal models to elucidate the pathophysiology of white matter damage and test treatments. [3] Glutamate-mediated excitotoxicity, inflammatory cytokines, and protease activation are thought to cause oligodendrocytes (Ol) death in acute ischemic injury, but little is known about the mechanisms of white matter injury in chronic vascular disease. [4] Damage to small vessels causes an inflammatory response with disruption of blood-brain barrier (BBB) and subsequent accumulation of fluid and macromolecules in white matter. [5] In animal models of hypoxic hypoperfusion, damage to the white matter is associated with disruption of the BBB, break down of myelin basic protein (MBP), and Ol cell death. [6]

Matrix metalloproteinases (MMPs) and tumor necrosis factor-α (TNF-α), which are increased in neuroinflammation, are implicated in MBP break down and Ol death. [7, 8] Brain tissues from vascular dementia patients show expression of MMPs in the regions of white matter damage. [9] Vascular cognitive impairment patients have disruption of the BBB suggestive of an inflammatory response. [10, 11] Studies of cerebrospinal fluid (CSF) show elevated MMPs. [12] In acute ischemia, there is early elevation of MMP-2. [13] Hypoxia-induced MMP-9 expression leads to vascular leakage. [14] Knockout of MMP-9 reduces BBB leakage in acute ischemia. [15] TNF-α production by microglia has been demonstrated to participate in Ol death in chronic cerebral hypoperfusion. [16]

Several animal models are used to study vascular cognitive impairment. Most commonly, bilateral carotid artery occlusion is performed in young normotensive rats, producing hypoxic hypoperfusion. [17] Since vascular cognitive impairment patients with white matter damage generally are elderly individuals with vascular disease secondary to hypertension and/or diabetes mellitus, a more appropriate animal model is an older spontaneously hypertensive-stroke prone rat (SHR-SP). These animals develop extensive white matter damage with gliosis, apoptosis of Ols, and BBB damage, but the role of neuroinflammation has not been determined. [18] We hypothesized that white matter injury is a neuroinflammatory process associated with expression of MMPs and cytokines. To study the role of inflammation in vascular cognitive impairment in an animal model, we used a 12-week old SHR-SP with a unilateral carotid artery occlusion (UCAO) and the Japanese permissive diet (JPD) with added salt in the water. We used MRI to monitor white matter injury and histological/biomedical studies to identify BBB opening, myelin loss, and Ol death and expression of neuroinflammatory proteases and cytokines. Morris water maze (MWM) was used to test for cognitive impairment.

Methods

A detailed description of methods is found in the supplement.

Animal groups and Surgery

All protocols followed the guidelines of the Institutional Animal Care and Use Committee (IACUC) at the University of New Mexico. SHR-SP rats were divided into two groups: i)

UCAO/JPD and ii) sham-operated. UCAO, as described in the Supporting Methods, was performed on 12-week-old male SHR-SP (Charles River Laboratories). Following UCAO, rats were placed on a JPD (18.7% protein, 0.63% potassium, 0.37% sodium; Ziegler Bros, Inc.) with 1 % sodium chloride added to drinking water for 4 or 5 weeks (end point was determined based on the appearance of neurological symptoms and white matter lesions on T2-weighted MRI). In the sham-operated group the right carotid artery was isolated and rats were fed with regular rodent diet with tap water following this procedure.

Physiological parameters

Body weight and systolic blood pressure (SBP) were recorded weekly. Plasma pH, pO_2, pCO_2, glucose, K^+, and Na^+ levels were also determined.

Histological Analysis

Klüver-Barrera (KB) and hematoxylin eosin (H & E) staining followed standard protocols. For immunohistochemistry (IHC) brain sections were stained using anti-MMP-2, anti-MMP-3, anti-MMP-9, anti-glial fibrillary acidic protein (GFAP), anti-cleaved caspase-3, anti-APC (CC1), anti-TNF-α, anti-Iba-1, and anti-Cy-3-conjugated Affinity Pure Goat Anti-Rat IgG antibodies.

Magnetic Resonance Imaging (MRI)

White matter lesions were evaluated using MRI (4.7-T small animal scanner; Bruker Biospin) weekly following the UCAO/JPD. Detailed descriptions of the method were reported previously. [19]

Immunoblotting

Western blotting followed standard techniques. Primary antibodies included anti-MBP, anti-GalC, anti-MMP-2, anti-MMP-3, anti-MMP-9, and anti-active caspase-3.

Evaluation of BBB permeability by IgG leakage

We used an ELISA kit (GenWay Biotech, Inc.) to measure the levels of brain tissue IgG.

Morris water maze

Three weeks following UCAO/JPD, cognitive function was assessed as reported previously. [20]

Statistical Analysis

Data are expressed as means ± S.E.M. Statistical significance was set at $P < 0.05$. Data were analyzed by two-way ANOVA followed by Bonferroni t-test analysis, and unpaired Student's t-tests, using Prism 5.0 (GraphPad Software Inc.).

Results

Baseline body weight was similar between UCAO/JPD and sham-operated groups. The UCAO/JPD group increased in body weight during the first week, but had a significant weight loss during weeks 3, 4, and 5 ($P < 0.01$). The sham-operated group gained in body weight throughout the course of the study (Supplementary Figure 1A).

SBP gradually increased in SHR-SP rats from 7 to 12 weeks of age, continuing to increase for 4 weeks post UCAO/JPD, and was significantly different on weeks 3 and 4 compared to sham group ($P < 0.001$, $P < 0.01$, respectively; Supplementary Figure 1B).

Blood chemistry parameters were not significantly different between groups (Supplementary Table 1).

Following 4-5 weeks of UCAO/JPD, there was a gradual increase in the number of rats developing neurological deficits including lethargy, absence of exploration, gait deficit, hemiparesis, and abnormal circling. T2-weighted images displayed hyperintense areas in the white matter and hippocampus in both hemispheres, and unilaterally in cortex. Sham-operated rats showed no T2 hyperintensities (Figure 1A).

Myelin loss, using Klüver-Barrera staining, was observed in the external capsule, corpus callosum, and internal capsule of both occluded and non-occluded sides 4-5 weeks following UCAO/JPD (Figure 1B). Most of the myelin loss occurred in a caudal portion of the brain (approximately -2 to -6 mm relative to Bregma). This damage was characterized by increased vacuolation and rarefaction of myelin fibers. No white matter damage was seen in the sham-operated group in either hemisphere. Western blot demonstrated that MBP was significantly decreased in the occluded side of external capsule and corpus callosum and in the non-occluded hemisphere in external capsule, corpus callosum, and internal capsule compared to corresponding control ($P < 0.05$; Figure 1C and D). Immunoblotting with GalC showed immature Ol increases in all three areas of white matter on the non-occluded side, and in corpus callosum and internal capsule of the occluded side (Figure 1C and D).

In MWM, rats that received UCAO/JPD demonstrated significantly higher escape latencies during the acquisition trials than the sham-operated group on days 3 and 4 ($P < 0.01$; Figure 2A).

In the probe trial, in which the platform was removed, rats were required to recall the location of the platform in the northwest quadrant (NWQ), relying on distal cues. Rats in the sham-operated group had intact memory, evidenced by greater time spent in the NWQ while the UCAO/JPD group spent significantly less time, revealing memory impairments ($P < 0.01$; Figure 2B).

Swimming speed during four days of the acquisition trial were similar (Figure 2C), indicating that deficits in performance by the UCAO/JPD group were not due to poor motor function. Additionally, there were no group differences in the latencies to find a platform with a visual cue, indicating that visual function was normal after UCAO/JPD (Figure 2D).

White matter IgG content was observed within the area of external capsule, and corpus callosum of the occluded side. Extravasations of IgG were also demonstrated in the regions of external capsule, corpus callosum, and internal capsule of the non-occluded side using ELISA (Figure 3A). In addition, MMP-9 was detected in the area of IgG leakage (Figure 3B). MMP-3 was not detected (data not shown). H & E staining showed hemorrhage and perivascular infiltrates of inflammatory-like cells. There was loss of structure in the white matter surrounding the vessels (Figure 3C).

Western blot showed that MMP-2 was present in both latent and active forms and was identified in both sham-operated and UCAO/JPD groups. MMP-2 was decreased in the external capsule on the non-occluded side following UCAO/JPD ($P < 0.001$) with no change detected on the occluded side (Figure 4A and B). We detected MMP-3 proform in both groups on both sides (Figure 4A and B). Western blot analysis showed a significant increase in the expression of proMMP-3 in areas of external capsule, corpus callosum and internal capsule in occluded ($P < 0.05$) and external capsule in non-occluded brain hemispheres ($P < 0.01$). ProMMP-9 was significantly greater in external capsule, corpus callosum, and internal capsule of the UCAO/JPD group on both sides when compared to the sham-operated group (Figure 4A and B). Strong co-localization of MMP-3 and MMP-9

immunoreactivity with GFAP and CC1 was observed (Figure 4C). No co-localization was observed with OX-42 (data not shown) suggesting that astrocytes and Ols are important sources of MMP-3 and MMP-9.

Confocal IHC images exhibited many cleaved caspase-3 positive cells in the area of external capsule, co-localized with CC1, suggesting that these Ols were undergoing apoptosis (Figure 5A). Western blot analysis demonstrated increased cleaved caspase-3 in the areas of external capsule, corpus callosum, and internal capsule of both hemispheres (Figure 5B and C). Sham-operated group showed little cleaved caspase-3. GFAP positive cells were distributed throughout white matter and hippocampus (Supplementary Figure 2A). TNF-α was increased in white matter and it was co-localized with Iba-1-positive microglia/macrophages (see insert Supplementary Figure 2B).

Discussion

This hypertensive rat model has damage to the white matter similar pathologically to that seen in vascular cognitive impairment patients. Our results indicate that inflammation with MMPs and TNF-α expression is associated with astrogliosis and death of mature Ols. At 12 weeks of age the SHR-SP were fed the JPD with salt in the drinking water and had a unilateral carotid occlusion. After 4 to 5 weeks, we found death of mature Ols, proliferation of immature Ols, breakdown of MBP, and opening of the BBB that was associated with an increase in MMPs. Memory impairment was demonstrated by MWM by week 3 following UCAO/JPD. Mature Ols expressed cleaved caspase-3 suggesting apoptosis. We observed an inflammatory response after UCAO/JPD that resulted in the expression of TNF-α in microglia and increased expression of MMP-3 and MMP-9 in reactive astrocytes and Ols. MMP-9 co-localized with regions where the BBB was disrupted as shown by IgG extravasation. These results support the hypothesis that inflammation is involved in white matter damage.

Although only one carotid was ligated, MRI showed white matter lesions in both hemispheres. A Prior study in young, normotensive rats used bilateral occlusion of the carotids to induce white matter damage. [21] When we attempted to occlude both carotids in the 12-week old SHR-SP, death occurred within 24 hours (data not shown). However, with occlusion of only one side, not only did the rats survive, but the injury pattern was apparent in both hemispheres, providing a model pathologically consistent with vascular cognitive impairment. Damage to the non-occluded hemisphere was greater than that seen in the occluded one. A previous study demonstrated that wall-to-lumen ratios of arteries from chronically hypertensive rats revert to those of normotensive rats when the vessels are ligated. [22] Further study will be needed to clarify the mechanism of apparent protection on the occluded side.

Extensive myelin disruption with marked decrease in MBP was seen by four weeks after the start of the diet and unilateral carotid occlusion. Ols showed increased expression of cleaved caspase-3 that co-localized with CC1. Mature Ols were targeted for cell death as revealed by the loss of the MBP, while immature Ols increased in number as shown by GalC. The damage to the myelin could have been due to a direct attack by the MMPs or loss of Ols leading to breakdown of the myelin sheath. The co-localization of MMP-9 with IgG supports its involvement in BBB disruption. MMP-3 was increased in cells close to the damaged myelin, but not in the vicinity of blood vessels. Our recent study supports the role of MMP-3 and MMP-9 in Ol death following cerebral ischemia. [7] MMP-2 including pro and active forms was decreased suggesting that MMP-2 may have been consumed. Thus, while MMP-3 and/or MMP-9 are most likely involved in the damage, MMP-2 may have contributed. [15, 23]

Our finding of extensive white matter damage in the SHR-SP with UCAO and JPD resemble the findings in pathological studies in vascular cognitive impairment patients with small vessel disease. [24, 25] The SHR-SP were studied between 12 and 16 weeks of life, making them a more relevant model for the human disease, which is seen mainly in elderly patients. Studies in human tissues show disruption of the BBB with expression of MMP-2 in reactive astrocytes and MMP-3 in pericytes. [9] MMP-3 and MMP-9 are increased in CSF of patients with vascular cognitive impairment. [12, 26]

Other injury pathways have been implicated in apoptotic death of Ols, such as oxidative stress, inflammation, or glutamate toxicity. [27] Previous studies demonstrated independent timing and mechanisms of Ol death versus demyelination, [28] which cannot be determined in our model. In demyelinating transgenic mouse, MMP-3 triggered neuroinflammation with microglial induction of TNF-α [29, 30] and MMP-3 up regulation preceded the onset of disease. [31] Release of MMP-3 from apoptotic neurons activated microglia and induced inflammatory cytokines, suggesting that MMP-3 may be a signaling molecule in neuronal apoptosis. [29] TNF-α and IL-1β produce a significant increase in the production of MMP-3 and MMP-9 in cultured astrocytes and microglia. Our data demonstrate that an increase in the expression of MMP-3 and MMP-9 parallel increased microglial reactivity, TNF-α expression, and eventual apoptotic death of Ols.

Hypertensive rats exhibiting white matter damage showed memory deficits in the MWM test by the third week after the UCAO/JPD, which was shown to be unrelated to either visual or motor deficits. Additionally, microglial activation that has been observed in the white matter in the present study may be involved in cognitive impairment. Since the hippocampus was involved in the injury, we cannot exclude a contribution to the memory loss from hippocampal damage which we plan to explore in future studies.

In conclusion, we have described a model of white matter damage in SHR-SP that has similarities to the hypertensive, small vessel form of vascular cognitive impairment seen in elderly patients. Our data show an inflammatory response, involving expression of MMPs and TNF-α with BBB opening and demyelination. This animal model combines the major features of small vessel vascular cognitive impairment and it exhibits not only myelin and Ol loss, but also cognitive impairment. The expression of MMPs and TNF-α in the regions of inflammatory damage to the BBB and Ols is consistent with earlier studies, but will have to be confirmed by blocking their action with inhibitors of MMPs. Because of its unique similarities to vascular cognitive impairment, this is a potential model for the study of agents to reduce the inflammatory response and slow progression of white matter damage.

Supplementary Material

Refer to Web version on PubMed Central for supplementary material.

Acknowledgments

Source of funding: This work was supported by grants from the National Institutes of Health (2 R01 NS045847-05A2).

References

1. Bowler JV. Modern concept of vascular cognitive impairment. Br Med Bull. 2007; 83:291–305. [PubMed: 17675645]
2. Chui H. Dementia due to subcortical ischemic vascular disease. Clin Cornerstone. 2001; 3:40–51. [PubMed: 11432121]

3. Hachinski V, Iadecola C, Petersen RC, Breteler MM, Nyenhuis DL, Black SE, et al. National institute of neurological disorders and stroke-canadian stroke network vascular cognitive impairment harmonization standards. Stroke. 2006; 37:2220–2241. [PubMed: 16917086]
4. Tekkok SB, Ye Z, Ransom BR. Excitotoxic mechanisms of ischemic injury in myelinated white matter. J Cereb Blood Flow Metab. 2007; 27:1540–1552. [PubMed: 17299453]
5. Pantoni L. Pathophysiology of age-related cerebral white matter changes. Cerebrovasc Dis. 2002; 13(2):7–10. [PubMed: 11901236]
6. Hainsworth AH, Markus HS. Do in vivo experimental models reflect human cerebral small vessel disease? A systematic review. J Cereb Blood Flow Metab. 2008; 28:1877–1891. [PubMed: 18698331]
7. Yang Y, Jalal FY, Thompson JF, Walker EJ, Candelario-Jalil E, Li L, et al. Tissue inhibitor of metalloproteinases-3 mediates the death of immature oligodendrocytes via TNF-α/TACE in focal cerebral ischemia in mice. J Neuroinflammation. 2011; 8:108. Epub ahead of print. [PubMed: 21871134]
8. Walker EJ, Rosenberg GA. Divergent role for mmp-2 in myelin breakdown and oligodendrocyte death following transient global ischemia. J Neurosci Res. 2010; 88:764–773. [PubMed: 19830840]
9. Rosenberg GA, Sullivan N, Esiri MM. White matter damage is associated with matrix metalloproteinases in vascular dementia. Stroke. 2001; 32:1162–1168. [PubMed: 11340226]
10. Taheri S, Gasparovic C, Huisa BN, Adair JC, Edmonds E, Prestopnik J, et al. Blood-brain barrier permeability abnormalities in vascular cognitive impairment. Stroke. 2011; 42:2158–2163. [PubMed: 21719768]
11. Topakian R, Barrick TR, Howe FA, Markus HS. Blood-brain barrier permeability is increased in normal-appearing white matter in patients with lacunar stroke and leucoaraiosis. J Neurol Neurosurg Psychiatry. 2010; 81:192–197. [PubMed: 19710048]
12. Candelario-Jalil E, Thompson J, Taheri S, Grossetete M, Adair JC, Edmonds E, et al. Matrix metalloproteinases are associated with increased blood-brain barrier opening in vascular cognitive impairment. Stroke. 2011; 42:1345–1350. [PubMed: 21454822]
13. Yang Y, Estrada EY, Thompson JF, Liu W, Rosenberg GA. Matrix metalloproteinase-mediated disruption of tight junction proteins in cerebral vessels is reversed by synthetic matrix metalloproteinase inhibitor in focal ischemia in rat. J Cereb Blood Flow Metab. 2007; 27:697–709. [PubMed: 16850029]
14. Bauer AT, Burgers HF, Rabie T, Marti HH. Matrix metalloproteinase-9 mediates hypoxia-induced vascular leakage in the brain via tight junction rearrangement. J Cereb Blood Flow Metab. 2010; 30:837–848. [PubMed: 19997118]
15. Asahi M, Wang X, Mori T, Sumii T, Jung JC, Moskowitz MA, et al. Effects of matrix metalloproteinase-9 gene knock-out on the proteolysis of blood-brain barrier and white matter components after cerebral ischemia. J Neurosci. 2001; 21:7724–7732. [PubMed: 11567062]
16. Masumura M, Hata R, Nagai Y, Sawada T. Oligodendroglial cell death with DNA fragmentation in the white matter under chronic cerebral hypoperfusion: Comparison between normotensive and spontaneously hypertensive rats. Neurosci Res. 2001; 39:401–412. [PubMed: 11274739]
17. Wakita H, Tomimoto H, Akiguchi I, Kimura J. Glial activation and white matter changes in the rat brain induced by chronic cerebral hypoperfusion: An immunohistochemical study. Acta Neuropathol. 1994; 87:484–492. [PubMed: 8059601]
18. Guerrini U, Sironi L, Tremoli E, Cimino M, Pollo B, Calvio AM, et al. New insights into brain damage in stroke-prone rats: A nuclear magnetic imaging study. Stroke. 2002; 33:825–830. [PubMed: 11872910]
19. Sood R, Taheri S, Estrada EY, Rosenberg GA. Quantitative evaluation of the effect of propylene glycol on bbb permeability. J Magn Reson Imaging. 2007; 25:39–47. [PubMed: 17173307]
20. Morris R. Developments of a water-maze procedure for studying spatial learning in the rat. J Neurosci Methods. 1984; 11:47–60. [PubMed: 6471907]
21. Sood R, Yang Y, Taheri S, Candelario-Jalil E, Estrada EY, Walker EJ, et al. Increased apparent diffusion coefficients on MRI linked with matrix metalloproteinases and edema in white matter after bilateral carotid artery occlusion in rats. J Cereb Blood Flow Metab. 2009; 29:308–316. [PubMed: 18941468]

22. Folkow B, Gurevich M, Hallback M, Lundgren Y, Weiss L. The hemodynamic consequences of regional hypotension in spontaneously hypertensive and normotensive rats. Acta Physiol Scand. 1971; 82:9A–10A.

23. Chen J, Cui X, Zacharek A, Cui Y, Roberts C, Chopp M. White matter damage and the effect of matrix metalloproteinases in type 2 diabetic mice after stroke. Stroke. 2011; 42:445–452. [PubMed: 21193743]

24. Gold G, Giannakopoulos P, Herrmann FR, Bouras C, Kovari E. Identification of alzheimer and vascular lesion thresholds for mixed dementia. Brain. 2007; 130:2830–2836. [PubMed: 17878206]

25. Schneider JA, Arvanitakis Z, Bang W, Bennett DA. Mixed brain pathologies account for most dementia cases in community-dwelling older persons. Neurology. 2007; 69:2197–2204. [PubMed: 17568013]

26. Adair JC, Charlie J, Dencoff JE, Kaye JA, Quinn JF, Camicioli RM, et al. Measurement of gelatinase b (mmp-9) in the cerebrospinal fluid of patients with vascular dementia and alzheimer disease. Stroke. 2004; 35:e159–162. [PubMed: 15105518]

27. Goldberg MP, Ransom BR. New light on white matter. Stroke. 2003; 34:330–332. [PubMed: 12574526]

28. Jamin N, Junier MP, Grannec G, Cadusseau J. Two temporal stages of oligodendroglial response to excitotoxic lesion in the gray matter of the adult rat brain. Exp Neurol. 2001; 172:17–28. [PubMed: 11681837]

29. Kim YS, Kim SS, Cho JJ, Choi DH, Hwang O, Shin DH, et al. Matrix metalloproteinase-3: A novel signaling proteinase from apoptotic neuronal cells that activates microglia. J Neurosci. 2005; 25:3701–3711. [PubMed: 15814801]

30. Choi DH, Kim EM, Son HJ, Joh TH, Kim YS, Kim D, et al. A novel intracellular role of matrix metalloproteinase-3 during apoptosis of dopaminergic cells. J Neurochem. 2008; 106:405–415. [PubMed: 18397366]

31. D'Souza CA, Mak B, Moscarello MA. The up-regulation of stromelysin-1 (mmp-3) in a spontaneously demyelinating transgenic mouse precedes onset of disease. J Biol Chem. 2002; 277:13589–13596. [PubMed: 11830584]

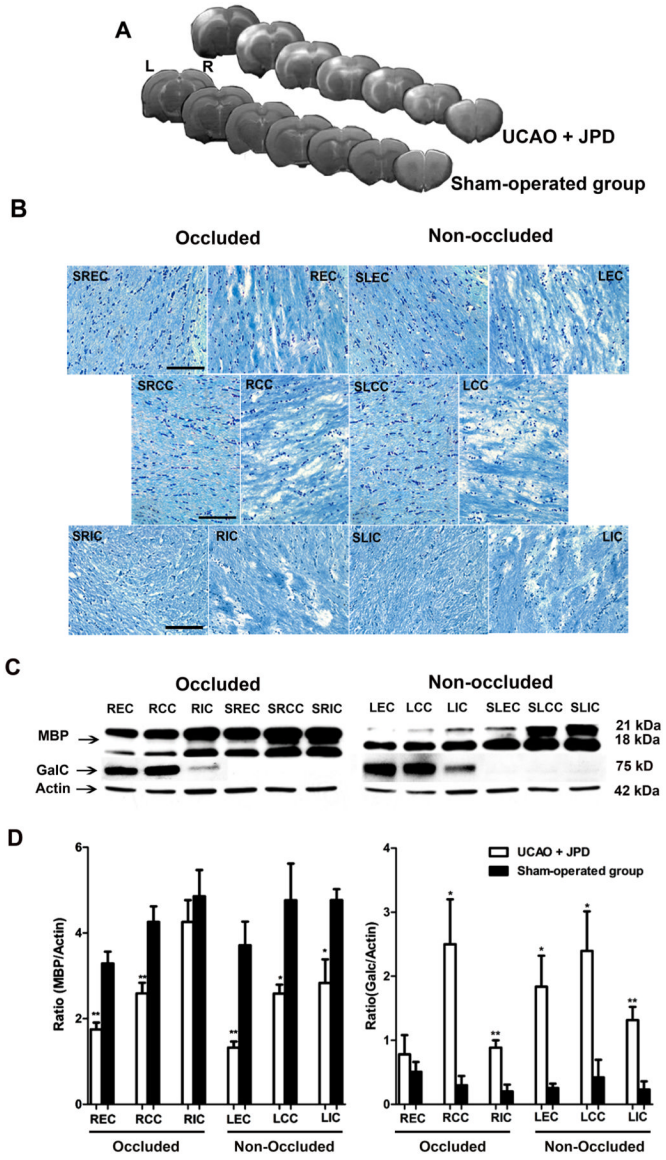

Figure 1.

Myelin loss and up-regulation of immature Ols seen at 4-5 weeks following UCAO and JPD. A) T2-weighted images obtained from UCAO/JPD and sham-operated groups demonstrate hyperintense areas on both occluded (R) and non-occluded (L) sides. An infarct seen in non-occluded cortex. B) Klüver-Barrera staining showed no damage in sham-operated group external capsule (SEC), corpus callosum (SCC), and internal capsule (SIC) in both hemispheres. UCAO/JPD rats had myelin and cell loss, as well as vacuolation, on both occluded and non-occluded sides of external capsule (EC), corpus callosum (CC), and internal capsule (IC). C) Representative blots of MBP and GalC for occluded and non-occluded sides of different areas of white matter. Actin was used as a loading control. D) Western blot densitometric analysis of MBP and GalC was normalized to actin. Scale bar=100μm. * $P < 0.05$, ** $P < 0.001$, significantly different compared to corresponding sham-operated control (S) (n=5/group).

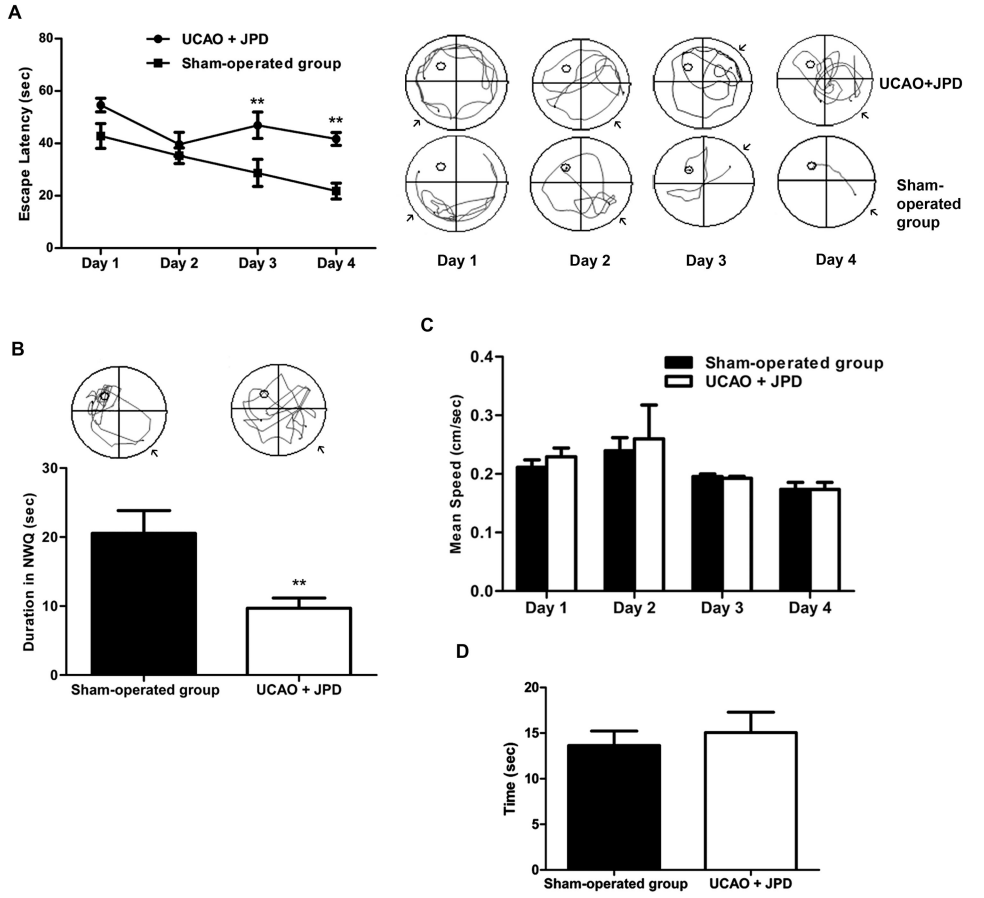

Figure 2.

Effect of UCAO/JPD on cognitive function in MWM. A) Histogram of latency to reach the hidden platform (left panel). Representative swim paths of UCAO/JPD and sham-operated groups during the acquisition performance (right panel), arrows illustrate the start position of each rat. B) Representative tracks of UCAO/JPD and sham-operated rats in probe trial test (upper panel). Histogram of probe trial shows significantly decreased time rats spent in NWQ by UCAO/JPD compared with the sham-operated group. C) Mean velocities (cm/sec) during the acquisition trial (days 1-4 of water maze study) of UCAO/JPD and sham-operated group. D) Cue test. The values represent mean ± S.E.M. ** $P < 0.01$ compared to sham operated group (n=9 in UCAO/JPD group, n=6 in sham-operated group).

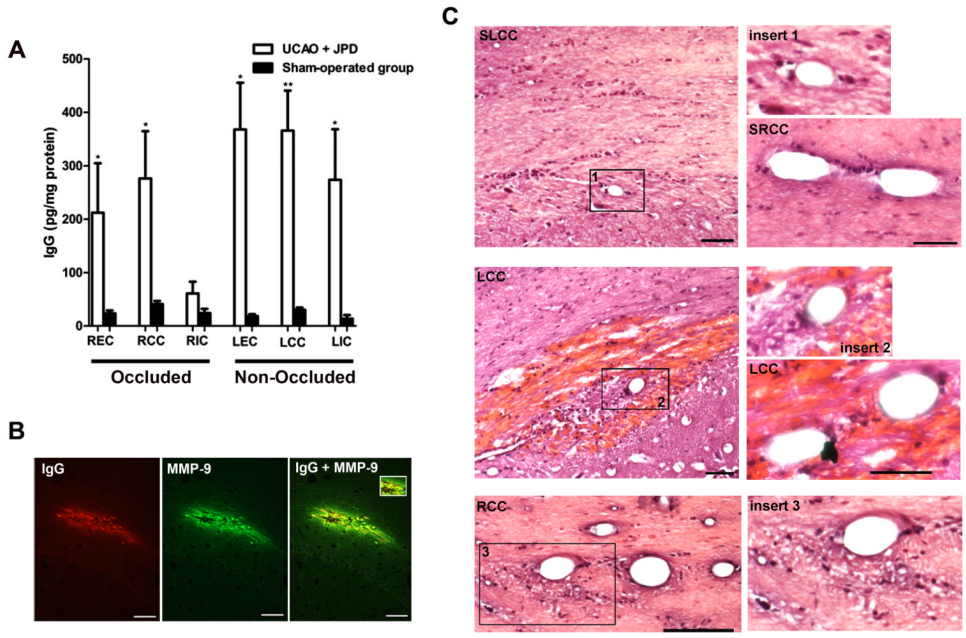

Figure 3.

Blood-brain barrier damage following UCAO/JPD. A) Quantification of IgG concentration by ELISA for both occluded (R) and non-occluded (L) sides of external capsule (EC), corpus callosum (CC), and internal capsule (IC). Values are expressed as mean ± S.E.M. B) Immunohistochemistry analysis shows IgG leakage from vessels in the CC of UCAO/JPD group, IgG was co-localized with MMP-9 (yellow). C) H&E-stained sections revealed hemorrhages surrounding vessels in the area of CC in UCAO/JPD group. No hemorrhage was seen in sham-operated group corpus callosum (SCC) (upper four panels). Perivascular infiltrate of inflammatory like cells in both occluded (R) and non-occluded (L) sides of CC following UCAO/JPD (lower four panels). Well maintained blood vessels in sham-operated control. Scale bar, 50 μm (right panels) and 100 μm (left panels). * $P < 0.05$, ** $P < 0.01$ compared with corresponding control (n=5/group).

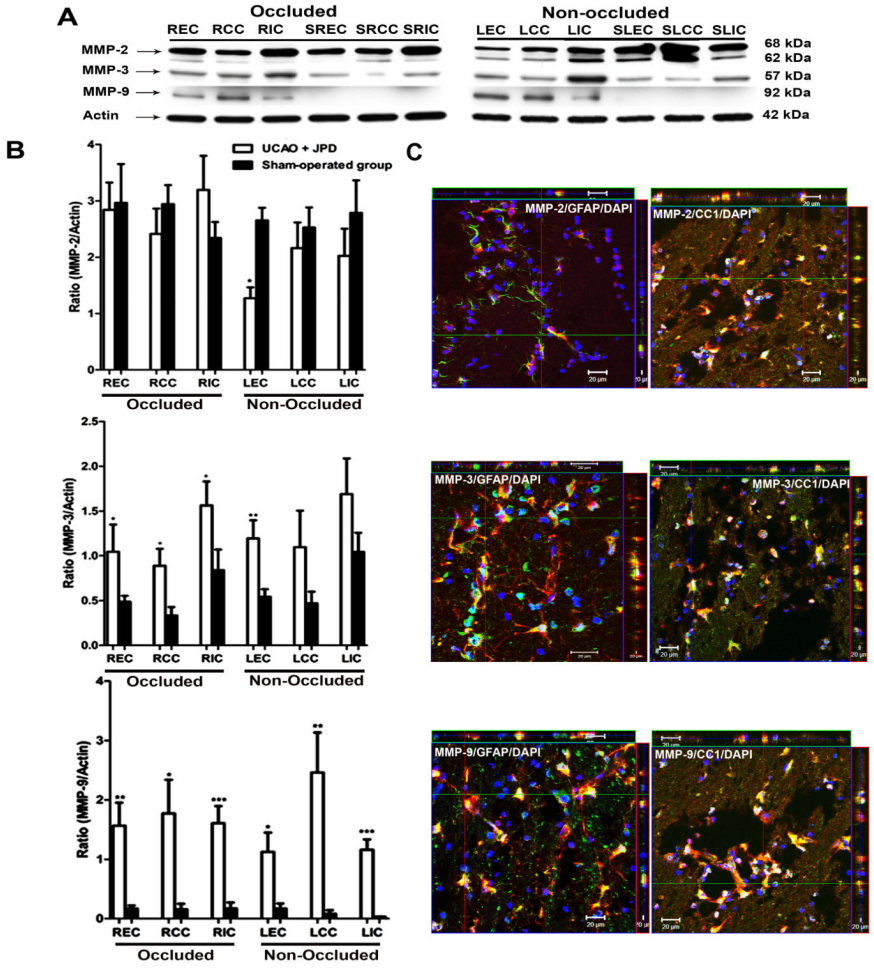

Figure 4.

Effect of UCAO/JPD on MMPs in white matter areas. A) Immunoblots of MMP-2, MMP-3, and MMP-9 from white matter extract of UCAO/JPD and sham-operated (S) groups in regions of external capsule (EC), corpus callosum (CC), and internal capsule (IC) from occluded (R) and non-occluded (L) sides. Actin was used as loading control (lower panel). B) Quantification of Western blot analysis for MMP-2, MMP-3, and MMP-9. C). Z-stack showing co-localization of astrocytes (GFAP) or Ols (CC1) and MMP-2, MMP-3, or MMP-9. Scale bar=20 μm. * $P < 0.05$, ** $P < 0.01$, *** $P < 0.001$ vs corresponding sham-operated group (n=5/group).

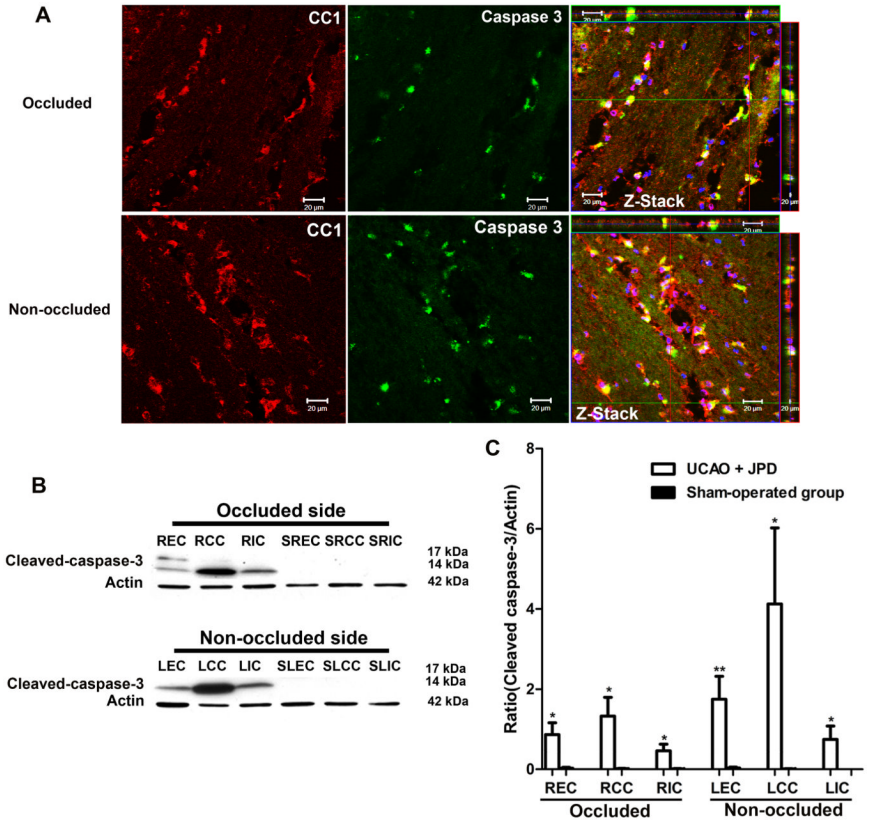

Figure 5.

Apoptotic death of Ols following UCAO/JPD. A) Cleaved caspase-3 (green), and mature Ols (CC1; red) positive cells in occluded and non-occluded sides. Yellow stains in Z-stack confocal images indicate co-localization of CC1 and cleaved caspase-3 positive cells. Scale bars=20 μm. B) Representative immunoblots of cleaved caspase-3 in occluded (R) and non-occluded (L) sides in the areas of external capsule (EC), corpus callosum (CC), and internal capsule (IC) of UCAO/JPD and sham-operated group (S). Actin was used as a loading control. C) Histogram representing cleaved caspase-3 expression measured using densitometric analysis. Data are expressed as the mean ± S.E.M. and normalized to actin (n = 6/group; * $P < 0.05$, ** $P < 0.01$).